Mechanical analysis and modeling of the efficiency of a road bicycle's power transmission system

Juan José González Oneto

2023-03-30

An analytical model for a bicycle's chain drive efficiency considering only frictional losses was analysed and implemented in the Julia programming language, resulting in the creation of the package `BicycleEfficiency.jl`. This model was reviewed and contrasted with experimental data, and was extended in order to increase it's accuracy. This work presents a novel approach to frictional losses by including an expression that allows the calculation of chain tension as a function of operating conditions and by taking into account the effects of chain tensioners.

Introduction

Road cycling is one of the most practiced and renowed sports in the world. As with practically any other modern sport, developing better equipment and improving the athelete's performance through science and engineering has become a major focus for professional and amateur riders alike.

One of such efforts is the design of optimal race strategies. This field of research revolves around developing mathematical models to simulate a cyclist's performance under different race conditions, which can then be analysed in order to identify the strategy that minmizes race time for a given track. Typically, these models aim to quantify power losses due to resistive forces such as aerodynamic drag, and to find their relationship with controllable parameters such as bicycle configuration, cyclist posture and power output. Examples of this type of work can be found in [1]–[4].

One of such sources of power loss is related to the efficiency of the bicycle's power transmission system. When developing models for race strategy optimization, it is a common practice to consider the chain drive's efficiency as a constant parameter obtained from direct measurements or from the literature [1]–[4]. This approach is both useful and practical, but has limited

interpretability in relation to the power transmission's system design and configuration. Hence, there exists an opportunity to improve race strategy optimization effort by developing models for the bycicle's chain drive system efficiency.

The purpose of this work is to examine currently available models as well as implement them computationally, in order to analyse their implications and shortcomings. Finally, a new model is proposed through the integration and adjustment of the different models found in the literature. The computational implementation was carried out using the Julia programming language, and its results can be found in the package `BicycleEfficiency.jl`. All calculations have been performed using this package and the code used to generate the figures found in this work has been included in order to facilitate reproducibility. The package's documentation contains instructions and information regarding its use and installation.

Frictional losses

Frictional work has been identified as one of the sources of energy loss in power transmission systems involving roller chains, such as the ones commonly found in road bicycles [5], [6]. Owing to the importance of this type of mechanisms in industrial settings, there has been extensive work related to the modeling of frictional losses. However, it has been noted that a bicyle's power transmission system differs significantly from those found in the industry due to its unique operating conditions, which include exposure to exteriors and chain misalignment [5], [7]. Thus, when modeling frictional losses on a bicycle's chain drive, only the models developed specifically for the derailleur-type systems found on road bicycles should be considered.

One of the earliest records of such efforts is found in the work of Spicer, Richardson, Ehrlich, Bernstein, Fukuda and Terada [5]. Their work seeked to study the effect of frictional losses on the efficiency of a bicycle's chain drive system and among their results is found an analytical model that allows the calculation of the efficiency for a variety of operating conditions and bicycle configurations, considering only power losses due to frictional work.

Analytical model

The model developed in [5] considered three sources of power loss: friction between inner link bushing and chain pin, chain line offset and contact between sprocket tooth, link roller and inner link bushing, and used the results obtained from the dynamic analysis performed on [7] to calculate chain tension, average tooth pressure angle and articulation angles.

Given that the purpose of this work is to analyse and implement the models computationally, a detailed description on how the model was developed will not be included. The reader is referred to the original source [5] for additional details and a more complete treatment on the development of the model.

Source 1: friction between inner link bushing and chain pin

As the name suggests, the first source of power loss comes from the relative motion that exists between chain pins and inner link bushing during chain articulation with the front and rear sprockets. It can be shown that power losses from this source can be calculated using the following expression.

$$P_1 = \frac{\pi}{2} T_0 N_1 \omega_1 \mu \rho (N_1^{-1} + N_2^{-1})$$

Where T_0 is chain tension, N_1 is the number of teeth on the front sprocket, ω_1 corresponds to pedaling cadence, μ is the coefficient of friction betweeen the pin and the bushing, ρ is the chain pin radius and N_2 is the number of teeth on the rear sprocket.

Source 2: chain line offset

As it was stated before, one of the unique features of a bicycle's chain drive is that the chain is misaligned most of the time due to the fact that it must accomodate different front and rear sprocket configurations. This implies that sprocket teeth slide against the inner part of the chain plates, which generates friction. Power losses through this mechanism are calculated as follows.

$$P_2 = N_1 \omega_1 \mu T_0 r_0 \sin(\gamma) (N_1^{-1} + N_2^{-1})$$

Two new variables have been introduced: r_0, which corresponds to the depth of sprocket teeth, and γ, which is the chain misalignment angle.

The reader will note that P_1 and P_2 are very similar. However, it should be noted that chain misalignment angle (γ) is typically very small, being approximately between 1 and 4 degrees [5], [7]. This means that $\sin(\gamma)$ will also be very small, and thus frictional losses from this source are almost negligible. This will be further explored in subsequent sections and can be visualized in Figure 1.

Source 3: sprocket tooth, link roller and inner link bushing

This source of power loss is related to the articulation and departure of the chain to the sprockets. In particular, it is noted that the chain's roller must rotate and slide in order to settle in its final position at the root of the sprocket. This motion generates friction between the roller and the bushing (roller rotates) and between the roller and the sprocket tooth (roller slides). Power losses due to this interaction can be modeled by the following equation.

$$P_3 = \frac{\mu T_0 r_R N_1 \omega_1}{4\pi} A \sum_{i=1}^{2} [\frac{2\pi}{N_i} \cos(\phi_i) - \sin(\phi_i) \ln(\cos(\frac{2\pi}{N_i}) + \sin(\frac{2\pi}{N_i}) \cot(\phi_i))]$$

Where the parameter A has the following definition

$$A = \frac{\delta\psi}{\pi - 1} \sum_{i=1}^{2} N_i$$

This equations have introduced new variables, such as r_R, which is the chain roller radius. Other variables, such as ϕ and δ can be related to known parameters. In particular, [7] presents the following relation to calculate ϕ.

$$\phi_i = 35 - \frac{120}{N_i}$$

It should the noted that the formula given for ϕ produces the angle in degrees. On the other hand, δ can be calculated with the following expression, given by [5].

$$\delta = \psi r_R$$

Where ψ is defined as the absolute roller rotation angle, which can be approximated as a constant parameter with a value of $\pi/2$.

Total power loss and efficiency

Total power loss can be determined through the sum of power losses from sources 1, 2 and 3.

$$P_{total} = P_1 + P_2 + P_3$$

Using this result, it is possible to determine the efficiency of the power transmission system, assuming that all power losses come from friction.

$$\eta = \frac{P_{out}}{P_{in}} = \frac{P_{in} - P_{total}}{P_{in}} = 1 - \frac{P_{total}}{P_{in}}$$

Model analysis

Using the model, it is possible to calculate not only the efficiency of the system, but also the magnitude power losses. This leads to one of the most interesting facts that can be derived from the model: power loss due to friction between inner link bushing and chain pin (source 1) is by far the most significant out of three sources of power loss considered in the model. Calculation over a range of commonly found operating conditions and sprocket configurations show that it typically accounts for approximately 90% of total power losses. As an example, Figure 1 shows the results obtained for a pedaling cadence of 80 rpm and a front-rear sprocket size relation of 50:21. It should be noted that parameters such as the friction coefficient, chain pitch and others needed for the calculation were partially taken from [5] and are listed in appendix A.

```
ω = 80*(2π/60)
N = [50, 21]

P1_80 = P1(μ, ρ, N, ω, T0)
P2_80 = P2(N, ω, μ, rR, γ, T0)
P3_80 = P3(μ, rR, N, ω, ψ, T0)

bar([P1_80, P2_80, P3_80], label=false, xlabel="Source",
    ylabel="Power [W]", xticks = [1, 2, 3], fillcolor = :lavender)
```

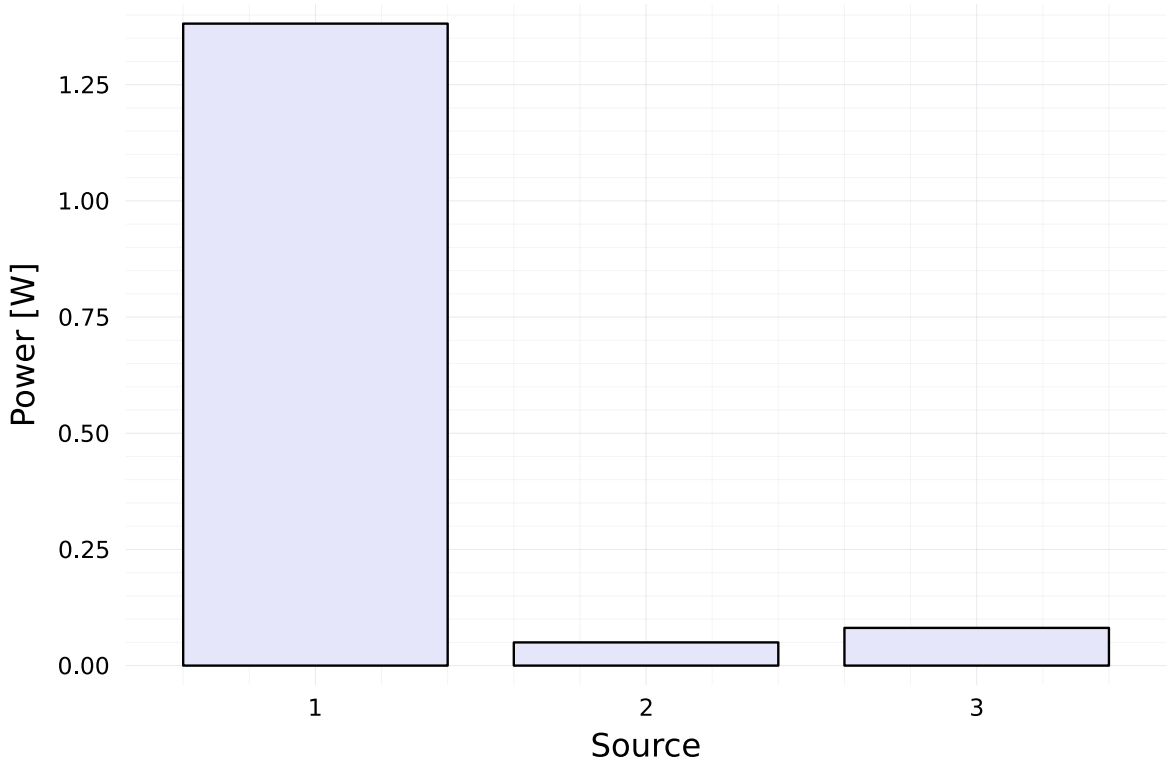

Figure 1: Power loss share

As it was stated before, Figure 1 shows that source 1 dominates overall power losses. For the particular case considered in Figure 1, friction between inner link bushing and chain pin accounts for 91.3% of power losses.

Another interesting aspect to explore through the model is the influence of sprocket size and pedaling cadence on power loss. Figure 2 shows power loss for various front and rear sprocket configurations as a function of pedaling cadence.

```
ω_rpm = 50:100
ω_rad = ω_rpm*(2*pi/60)
N1loss = [48, 52]
N2loss = [11, 34]

Ploss = [Ptotal(fill(μ, 3), p, ρ, ψ, rR, [i1, i2], j, γ, T0)
         for i1 in N1loss for i2 in N2loss for j in ω_rad]

shape = (length(ω_rad), length(N1loss) + length(N2loss))
```

```
labels = reshape(["$(i):$(j)" for i in N1loss for j in N2loss],
                 (1, length(N1loss) + length(N2loss)))

plot(ω_rpm, reshape(Ploss, shape), xlabel="Pedaling cadence [rpm]",
     ylabel="Power loss [W]", labels = labels, legend = :topleft)
```

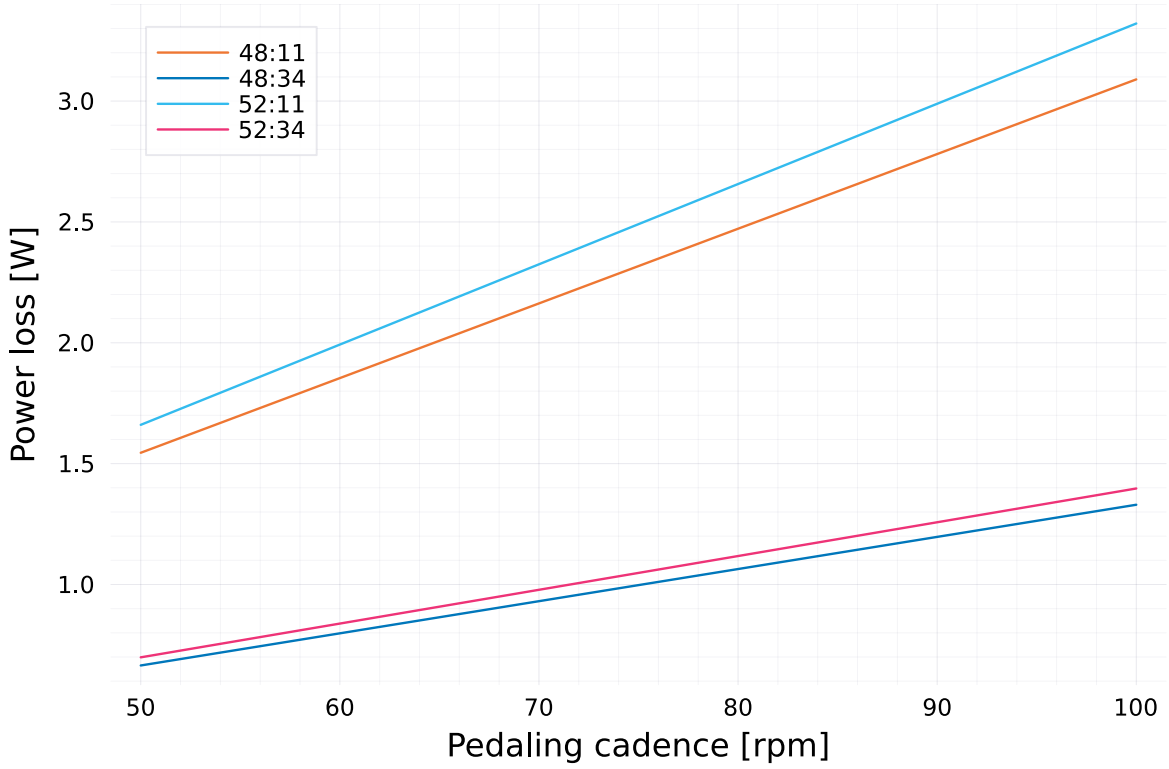

Figure 2: Power loss as a function of pedaling cadence for various sprocket configurations

Figure 2 shows that power loss increases linearly with pedaling cadence, and that increasing front sprocket size increases power losses, but increasing rear sprocket size has the oppposite effect. Another important conclusion that can be drawn from Figure 2 is that changes on rear sprocket size have a much more significant impact than changes on front sprocket size. This last behaviour is also exhibited when considering efficiency instead of power losses. Figure 3 shows the efficiency for different front and rear sprocket sizes, at 80 rpm.

```
N1_plot = [48, 50, 52]
N2_plot = [11, 21, 34]
```

```julia
η_plot = []
for i in N1_plot
    for j in N2_plot
        push!(η_plot, η(fill(μ, 3), p, ρ, ψ, rR, [i, j], ω, γ, T0)*100)
    end
end

bar(Float64.(η_plot), xlabel="Sprocket sizes", ylabel="Efficiency [%]",
    label=false, fillcolor=:lavender)
xticks!(1:9, ["$(i):$(j)" for i in N1_plot for j in N2_plot])
ylims!(97, 100)
```

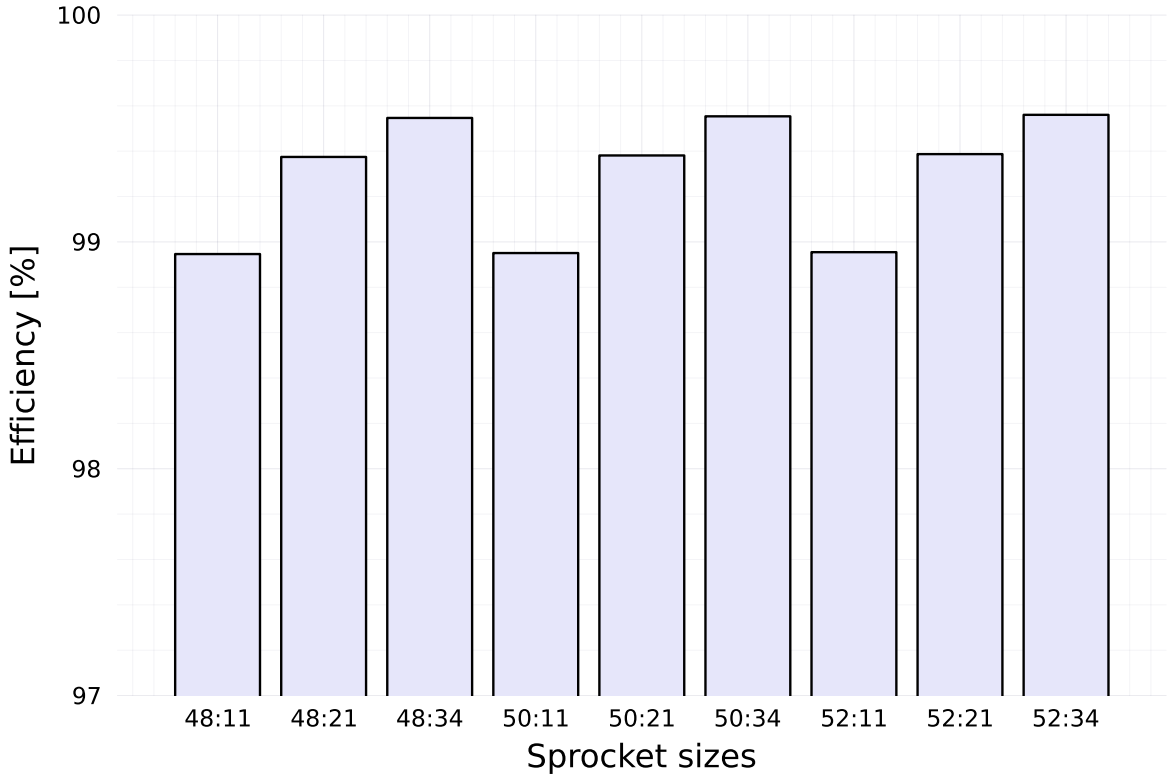

Figure 3: Influence of sprocket size on efficiency

Figure 3 shows that changes on front sprocket size have a marginal effect on efficiency, but changes on rear sprocket size can have more significant effects on efficiency. This effect is more evident in Figure 4, where it can be seen that increasing rear sprocket size from 11 teeth to 34 teeth can carry along an increase of 0.7% in efficiency. This result agrees with what was shown in Figure 2, which illustrates that power losses are reduced when the rear sprocket size

is increased. Figure 4 explores this relationship in further detail, by presenting the calculation of efficiencies for various rear sprocket sizes, keeping the front sprocket size constant at 50 teeth and pedaling cadence at 80 rpm.

```
N2_ef_rear = [11, 13, 15, 17, 19, 21, 23, 25, 27, 30, 34]
η_rear = [η(fill(μ, 3), p, ρ, ψ, rR, [50, i], ω, γ, T0)*100
            for i in N2_ef_rear]

bar(η_rear, label=false, xlabel="Rear sprocket size", ylabel="Efficiency [%]",
    fillcolor=:lavender, xticks=(1:length(N2_ef_rear), N2_ef_rear))
ylims!(97, 100)
```

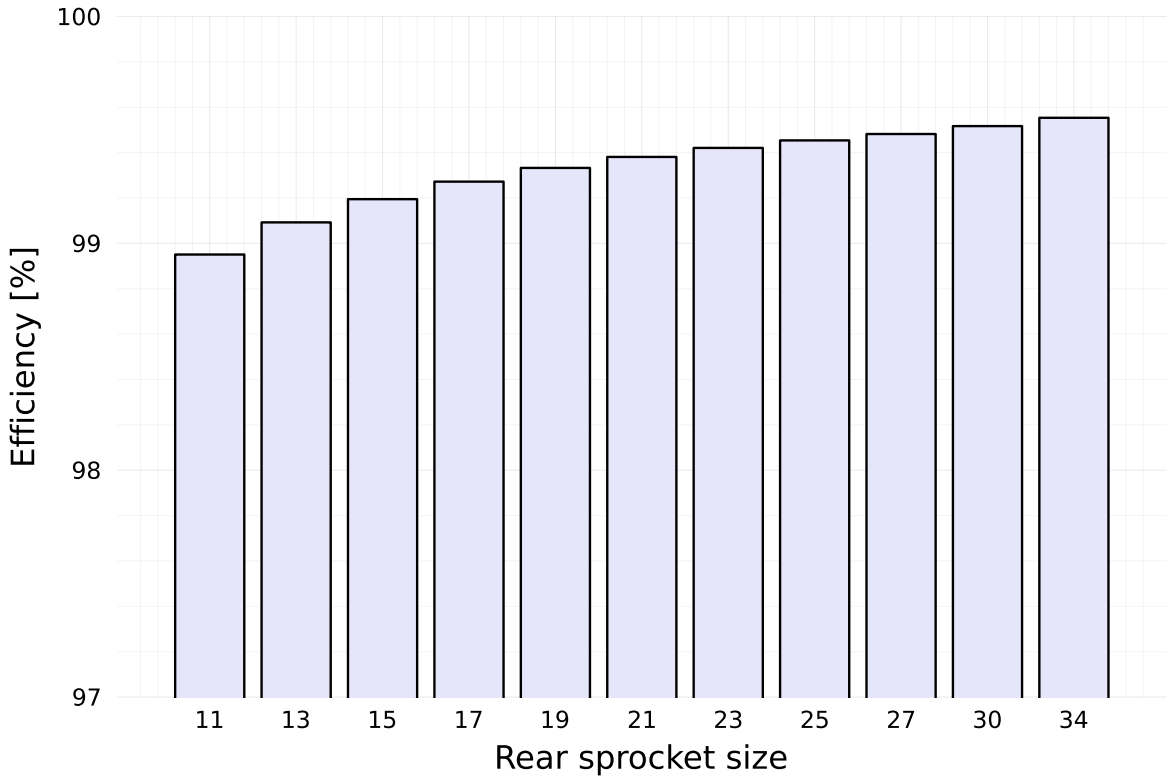

Figure 4: Rear sprocket size effect on efficiency (front sprocket size of 50 teeth)

Model validation

In addition to the model described above, [5] includes efficiency measurements under various operating conditions. This is used to contrast the behaviour predicted by the model with experimental results and to check the accuracy of power loss estimates. Table 1 shows estimated

efficiencies and their experimental counterparts for different pedaling speeds, at a fixed power input of 100 W and a sprocket relation of 52:21.

Table 1: Frictional losses model validation

Pedaling cadence [rpm]	Measured efficiency [%]	Calculated efficiency [%]	Error [%]
40	97.8	99.4	1.6
50	95.9	99.4	3.6
60	94.4	99.4	5.3
70	92.8	99.4	7.1
80	91.3	99.4	8.9
90	89.9	99.4	10.6

Table 1 shows that calculated efficiencies differ from those obtained through experimental measurements. In particular, it can be seen that the model predicts higher efficiencies than observed and that it doesn't account for variations in pedaling cadence, which seem to significantly affect efficiency.

On the other hand, the model discussed above presents a series of shortcomings related to chain tension. One of them is the fact that chain tension is modeled as a constant parameter that is independent of operating conditions and bicycle configuration. Examination of the literature regarding chain drive systems, such as [8], reveal that this assumption does not hold true, and that chain tension has a strong dependence on parameters such as power input and pedaling cadence. The following section will focus on this issue.

Another issue that can be found in the model is the fact that it only accounts for losses on the rear and front sprocket, which is not completely accurate, since a road's bicycle derailleur unit involves the presence of two additional sprockets. The effect of the presence of this mechanism is expected to increase power losses and will be explored in subsequent sections.

Chain tension

The models discussed previously all consider chain tension as a fixed parameter that might be related to bicycle configuration and operating conditions, but no expressions are given to calculate its value or understand its relationship with other parameters. A review of the literature regarding chain drive systems shows that chain tension can be related to chain and sprocket geometry (bicycle configuration) and to operating conditions such as power input [8]. This section presents a model developed to estimate chain tension as a function of current operating conditions, in an effort to increase model accuracy and reduce the number of assumptions and parameters needed to calculate efficiency.

First, it should be noted that chain tension comes from two sources mainly: centrifugal force and the forces exerted by the sprockets to the chain [8]. Figure 5 shows the chain (represented as small circles) and the front sprocket (big circle) and the variables involved in the calculation of chain tension due to sprocket forces.

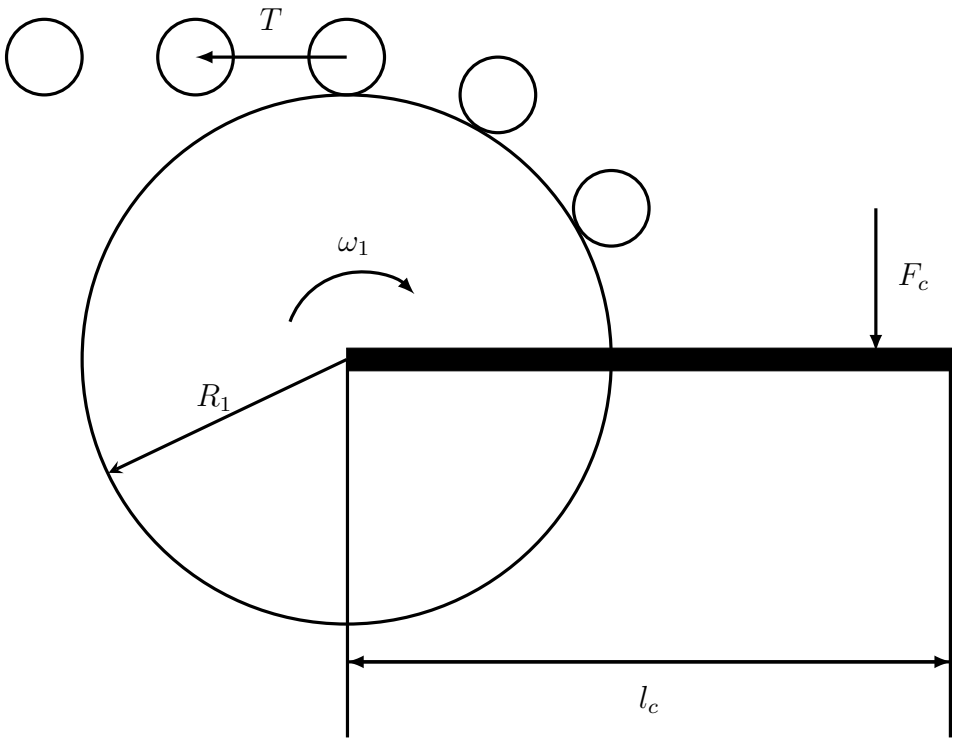

Figure 5: Chain tension due to force exerted by the sprockets

Following the notation used in Figure 5, T corresponds to chain tension, ω_1 is pedaling cadence, R_1 is the pitch radius of the front sprocket, l_c is the length of the crank and F_c is the force applied to the crank by the cyclist during pedaling.

Figure 5 shows that the force applied to the crank by the pedalist generates torque on the front sprocket, which is given by the following expression.

$$\tau = l_c F_c$$

This torque is transmitted to the front sprocket, which then exerts a force to the chain through its teeth. This force is perceived by the chain as tension and can be calculated using the torque on the front sprocket and it's pitch radius.

$$T = \frac{\tau}{R_1} = \frac{l_c F_c}{R_1}$$

Crank length and the force exerted by the cyclist to the pedals are not commonly known. Thus, it is more useful to express this result in terms of power input and pedaling cadence, which are much more commonly estimated and used by cyclists in pacing strategies. Observing that power input can be calculated as torque times pedaling cadence, the following results are obtained.

$$P_{in} = l_c F_c \omega_1$$

$$\frac{P_{in}}{\omega_1} = l_c F_c$$

Substituting this expression on the formula for chain tension (T) yields the following relationship.

$$T = \frac{P_{in}}{R_1 \omega_1}$$

The front sprocket's pitch diameter can be calculated using the following formula.

$$PD = \frac{p}{\sin(\pi / N_1)}$$

Where p corresponds to the chain pitch. Noting that $\pi << N_1$ for commonly found front sprocket sizes cycling, and that pitch radius is one half of the pitch diameter, the following expression is obtained for the pitch radius.

$$R_1 = \frac{pN_1}{2\pi}$$

This result allows the following formulation for chain tension due to the force exerted by the sprocket.

$$T = \frac{2\pi P_{in}}{\omega_1 p N_1}$$

The other component of chain tension, which is caused by centrifugal force, can be calculated using the following expression [8].

$$T_c = mv^2$$

Where m is the linear density of the chain (mass per unit length) and v is its velocity, which can be calculated from pedaling cadence and sprocket pitch radius as $\omega_1 R_1$. Substituting this

expression for v and using the result obtained above of R_1, tension due to centrifugal forces can be calculated as follows.

$$T_c = \frac{m(\omega_1 p N_1)^2}{4\pi^2}$$

Lastly, total chain tension can be determined by the sum of the tension due to the force exerted by the sprockets and the tension due to centrifigual forces. This produces the following result.

$$T_0 = \frac{2\pi P_{in}}{\omega_1 p N_1} + \frac{m(\omega_1 p N_1)^2}{4\pi^2}$$

This result shows that chain tension is a dynamic parameter that depends on riding conditions such as power input and pedaling cadence, and that it also depends on parameters related to the bicycle's geometry and configuration, such as front sprocket size and chain pitch. This equation can be used to calculate chain tension in the models described above, instead of passing it as a constant parameter, which should allow to produce more accurate predictions and model behaviour.

Lastly, Figure 6 shows chain tension as a function of power input, for a fixed pedaling cadence of 80 rpm and a range of front sprocket sizes.

```
N = 46:2:52
P_plot = 100:350

Tplot = [T(i, ω, p, j, m) for j in N for i in P_plot]

plot(P_plot, reshape(Tplot, (length(P_plot), length(N))),
     xlabel="Power input [W]", ylabel="Chain tension [N]",
     label=reshape(N, (1,length(N))), legend=:topleft)
```

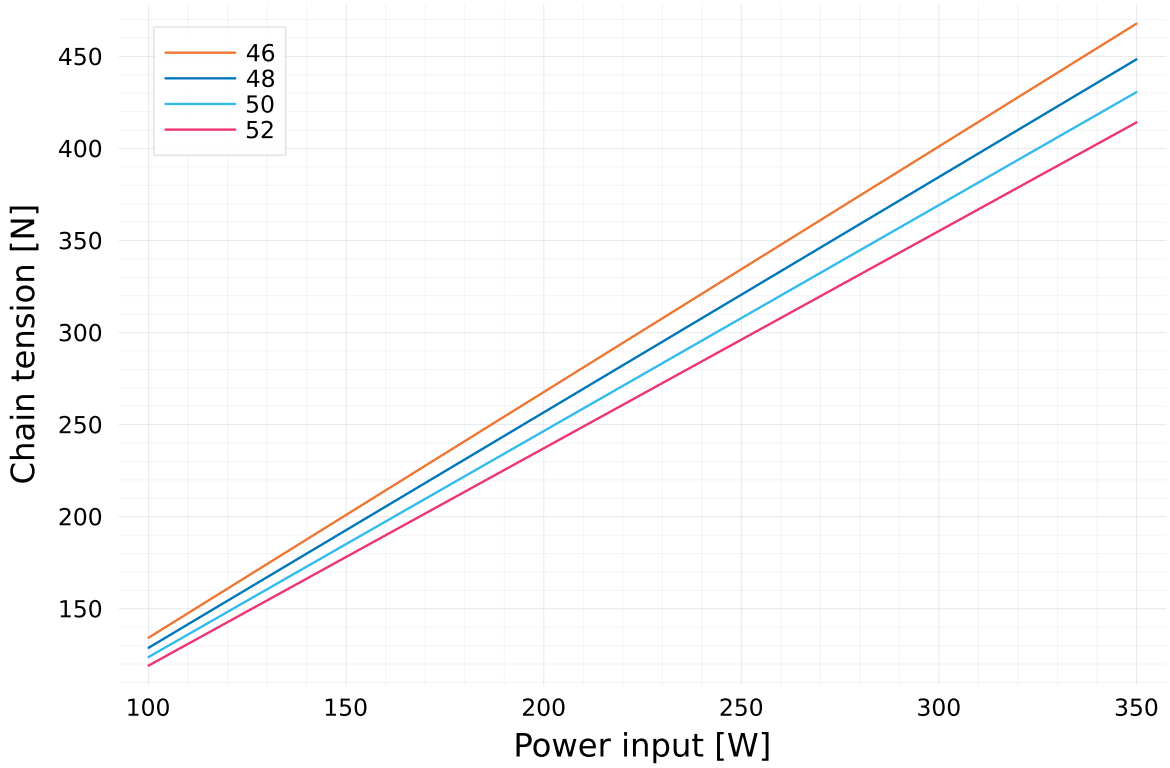

Figure 6: Chain tension as a function of power input for a pedaling cadence of 80 rpm

Figure 6 shows that chain tension in is the range of 100 to 450 N for common cycling conditions, which is in agreement to the values presented in [5]. Moreover, it shows that tension increases linearly with power input for a given pedaling cadence, which is to be expected, since increasing power input at a fixed pedaling cadence implies that a greater force is being applied to the pedals. Finally, it can also be seen that chain tension increases when front sprocket size decreases.

Chain tensioner

One of the unique characteristics of a road bicycle's chain drive system is the presence of a mechanism known as the chain tensioner. Given the fact that bicycles are equipped with multiple sprocket configurations ranging a wide variety of sizes, it is necessary to have a mechanism that ensures that the chain won't be too tensioned when the current configuration involves high sprocket sizes, and that it won't become slack when sprockets sizes are low. This mechanism is part of the derrailleur unit, and usually involves the addition of two small sprockets under the rear sprocket. These two sprockets are attached to a mechanical arm

which can move away or towards the front sprocket, and thus modify the distance that must be accommodated by the chain (for a fixed chain length, chain tension increases as the distance covered by the chain increases).

Since frictional losses are associated with the engaging and departure of the chain from the sprockets, the addition of two extra sprockets through the chain tensioner should increase power losses and decrease overall system efficiency. These effects become particularly important when considering that the sprockets in chain tensioners are typically small, which creates high articulation angles and increases frictional work between inner link bushing and chain pins (source 1 in frictional losses section). As it was previously shown in Figure 1, source 1 dominates overall power losses, so including the effect from the chain tensioner's sprockets should have a significant effect on efficiency calculations. Also, it was shown in Table 1 that calculated efficiencies are higher than their measured counterparts, so including the contributions from these sprockets should increase model accuracy.

Modifiying the equation for source one can be done by adding the contributions of the sprockets in the tensioner. This results in the following expression.

$$P_1 = \frac{\pi}{2} T_0 N_1 \omega_1 \mu \rho \sum_{i=1}^{4} \frac{1}{N_i}$$

It should be noted that the expression $(N_1^{-1} + N_2^{-1})$ has been replaced by a summation. This expression would be identical to the one reported above if the summation went up to N_2, however, the two extra terms added (N_3 and N_4) take into account the size of the sprockets in the tensioner.

Even though frictional losses are mostly due to source 1, equations for sources 2 and 3 can also be adjusted to include the effects of the tensioner. Noting that the expressions for sources 1 and 2 are very similar, the adjustment for source 2 also consists in adding the contribution of each sprocket.

$$P_2 = N_1 \omega_1 \mu T_0 r_0 \sin(\gamma) \sum_{i=1}^{4} \frac{1}{N_i}$$

Lastly, frictional losses associated to source 3 can also be adjusted to include the effects of the chain tensioner. The resulting expression has the following form.

$$P_3 = \frac{\mu T_0 r_R N_1 \omega_1}{4\pi} A \sum_{i=1}^{4} [\frac{2\pi}{N_i} \cos(\phi_i) - \sin(\phi_i) \ln(\cos(\frac{2\pi}{N_i}) + \sin(\frac{2\pi}{N_i}) \cot(\phi_i))]$$

This time, the parameter A has the following definition.

$$A = \frac{\delta\psi}{\pi - 1} \sum_{i=1}^{4} N_i$$

Frictional losses revisited

The results obtained for chain tension as a function of operating conditions and the adjustments made to include the effect of the chain tensioner on the model for frictional losses will be incorporated to generate a new analysis of frictional losses. In order to study the effect of these modifications, the analysis made for the original model (presented above) will be replicated.

First, power loss share will be evaluated to determine if changes made to the model altered the distribution of power losses among the 3 sources considered. Figure 7 shows the results for identical operating conditions as Figure 1. In both cases, power input was considered to be 250 W.

```
N = [50, 21, 12, 12]

P1_80 = P1T(Pin, μ, ρ, N, ω, m, p)
P2_80 = P2T(Pin, N, ω, μ, rR, γ, m, p)
P3_80 = P3T(Pin, μ, rR, N, ω, ψ, m, p)

bar([P1_80, P2_80, P3_80], label=false, xlabel="Source",
    ylabel="Power [W]", xticks=[1, 2, 3], fillcolor=:lavender)
```

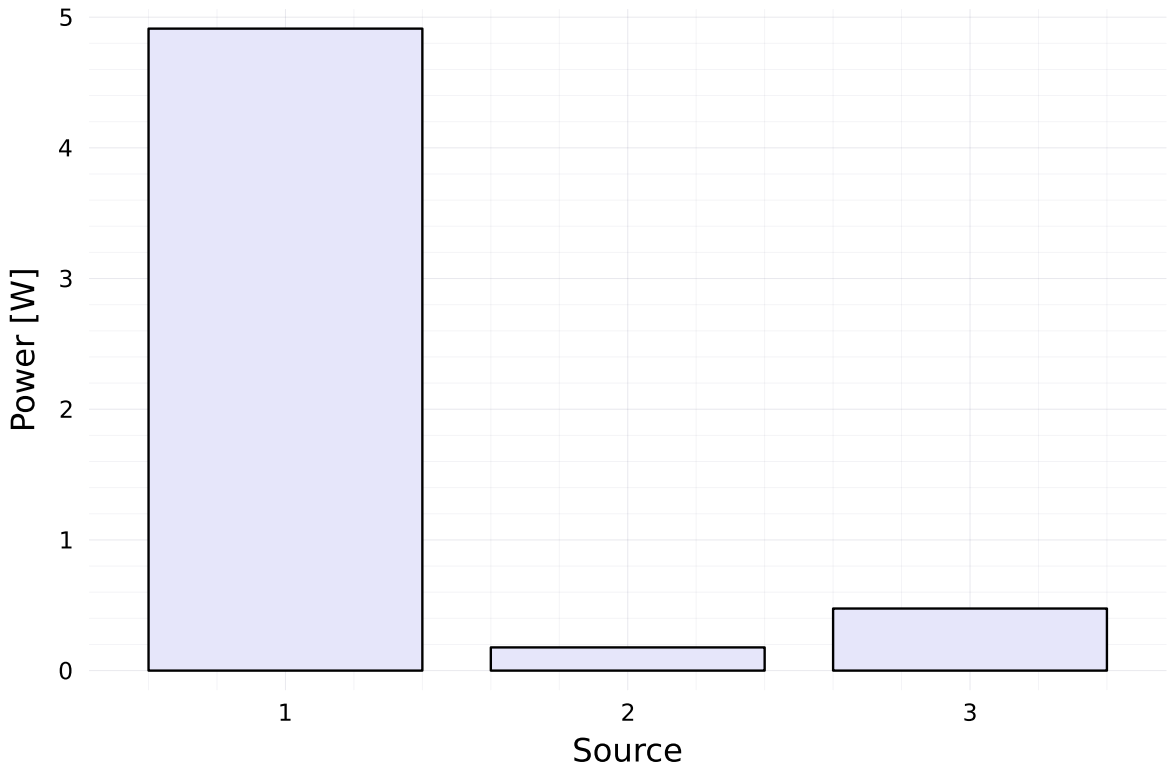

Figure 7: Power loss share with adjusted model

In this case, source 1 accounts for 88.3% of total power losses, which is slightly less than the value obtained for the original model. However, it can still be seen that power total power loss comes mostly from source 1.

Another aspect that is interesting to evaluate is the dependence of power losses on sprocket configuration and pedaling cadence. This was done in Figure 2 for the original model, and Figure 8 shows the results obtained for the new model, under the same operating conditions.

```
Ploss = [PtotalT(Pin, fill(μ, 3), p, ρ, ψ, rR, [i1, i2, 12, 12], j, γ, m)
         for i1 in N1loss for i2 in N2loss for j in ω_rad]

plot(ω_rpm, reshape(Ploss, shape), xlabel="Pedaling cadence [rpm]",
     ylabel="Power loss [W]", labels=labels, legend=:topleft)
```

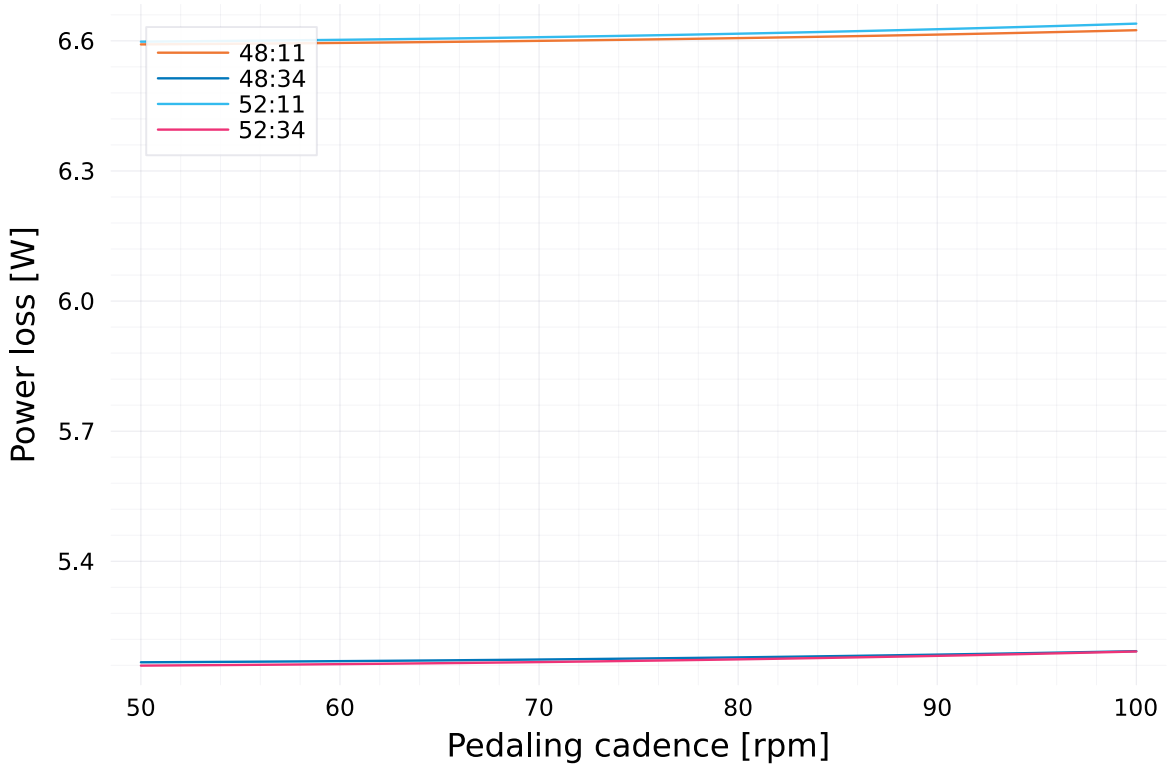

Figure 8: Power loss as a function of pedaling cadence for various sprocket configurations, adjusted model

Figure 8 shows that the adjustments have introduced a change on the model's behaviour. In particular, it can be observed that power losses are now virtually constant with respect to pedaling cadence. This can be explained by the fact that it was shown that chain tension is mainly due to the force exerted by the sprocket teeth to the chain (the contribution of centrifgual forces is abour 1%), which is inversely proportional to pedaling cadence. A closer examination of the curves presented in Figure 8 reveals that power losses are not constant with respect to pedaling cadence, since the term related to centrifugal forces is proportional to the second power of pedaling candece. Figure 9 shows total power losses only for the 48:34 sprocket relation.

```
Ploss = [PtotalT(Pin, fill(μ, 3), p, ρ, ψ, rR, [48, 34, 12, 12], i, γ, m)
         for i in ω_rad]

plot(ω_rpm, Ploss, xlabel="Pedaling cadence [rpm]",
     ylabel="Power loss [W]", label=false)
```

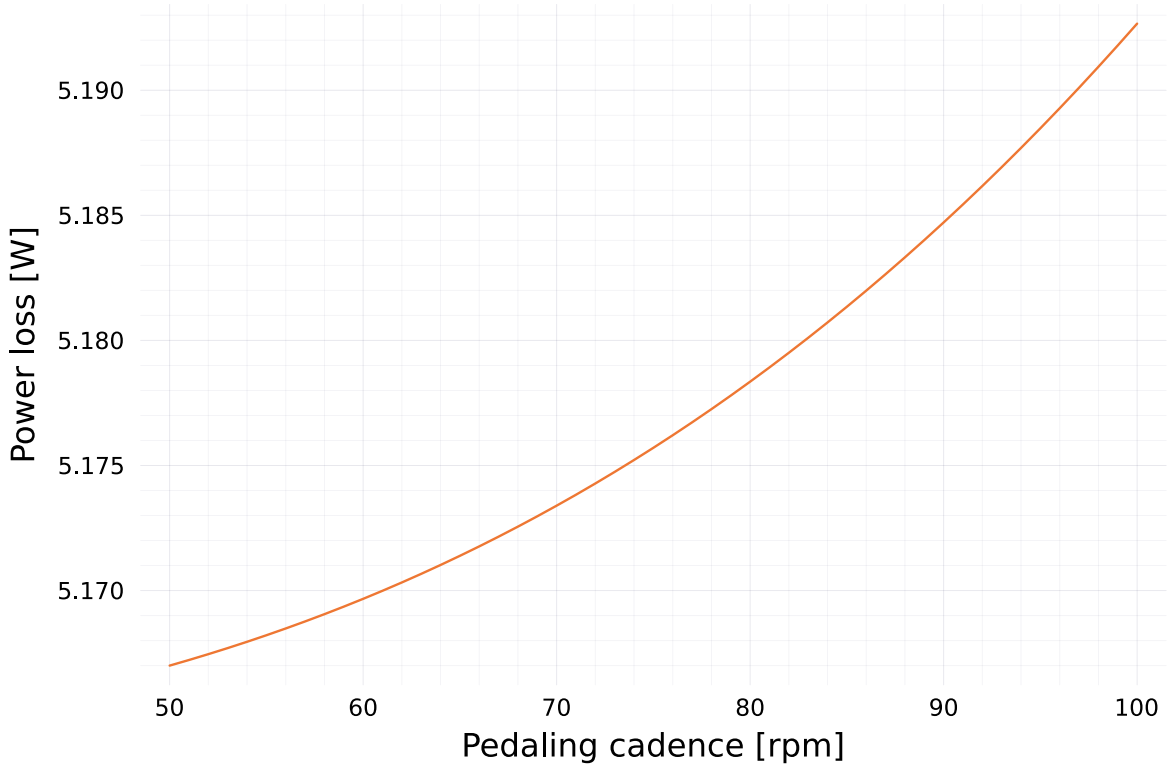

Figure 9: Power loss as a function of pedaling cadence for a sprocket relation of 48:34, adjusted model

Figure 9 shows power losses tend to increase with pedaling cadence, but that this effect is barely noticeable under common operating conditions.

It is also interesting to note that, once again, rear sprocket size has a much more dramatic effect on power losses (and efficiency) than front sprocket size. This claim is supported by Figure 8, where it can be seen that power losses increase significantly when rear sprocket size is reduced. This means that the dependence of efficiency on rear sprocket size should remain approximately equal, with the only difference that calculated efficiencies should be lower than before. Figure 10 shows calculated efficiencies for a variety of rear sprocket sizes, keeping front sprocket size at 50 teeth and pedaling cadence at 80 rpm.

```
η_rear2 = [ηT(Pin, fill(μ, 3), p, ρ, ψ, rR, [50, i, 12, 12], ω, γ, m)*100
           for i in N2_ef_rear]

bar(η_rear2, label=false, xlabel="Rear sprocket size", ylabel="Efficiency [%]",
    fillcolor=:lavender, xticks=(1:length(N2_ef_rear), N2_ef_rear))
```

```
ylims!(96.5, 98)
```

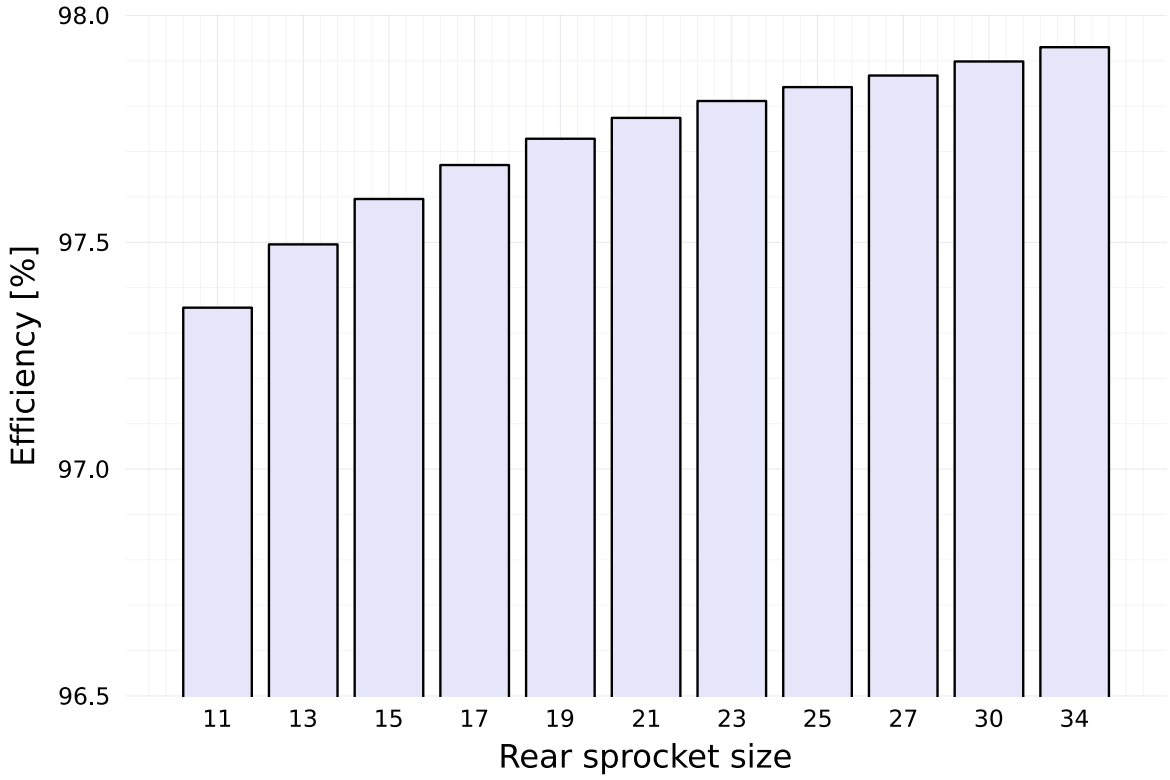

Figure 10: Rear sprocket size effect on efficiency (front sprocket size of 50 teeth), adjusted model

Figure 10 shows that including the effects of the chain tensioner produced a decrease of about 1.6% in calculated efficiencies for all rear sprocket sizes, which were mostly over 99% in the original model and are now all under 98%.

As it was mentioned before, one the of the shortcomings observed in the original model is that it predicts that efficiency is independent of pedaling cadence. Since chain tension is now a function of pedaling cadence and the behaviour of power losses with respect to this parameter has changes, it is expected that the relationship between efficency and pedaling cadence will be modified. Figure 11 explores this outcome.

```
ω_rpm = 50:150
ω_rad = ω_rpm*(2*pi/60)

η_pc = [ηT(Pin, fill(μ, 3), p, ρ, ψ, rR, [52, 21, 12, 12], i, γ, m)*100
```

```
            for i in ω_rad]

plot(ω_rpm, η_pc, label=false, xlabel="Pedaling cadence [rpm]", ylabel="Efficency [%]")
```

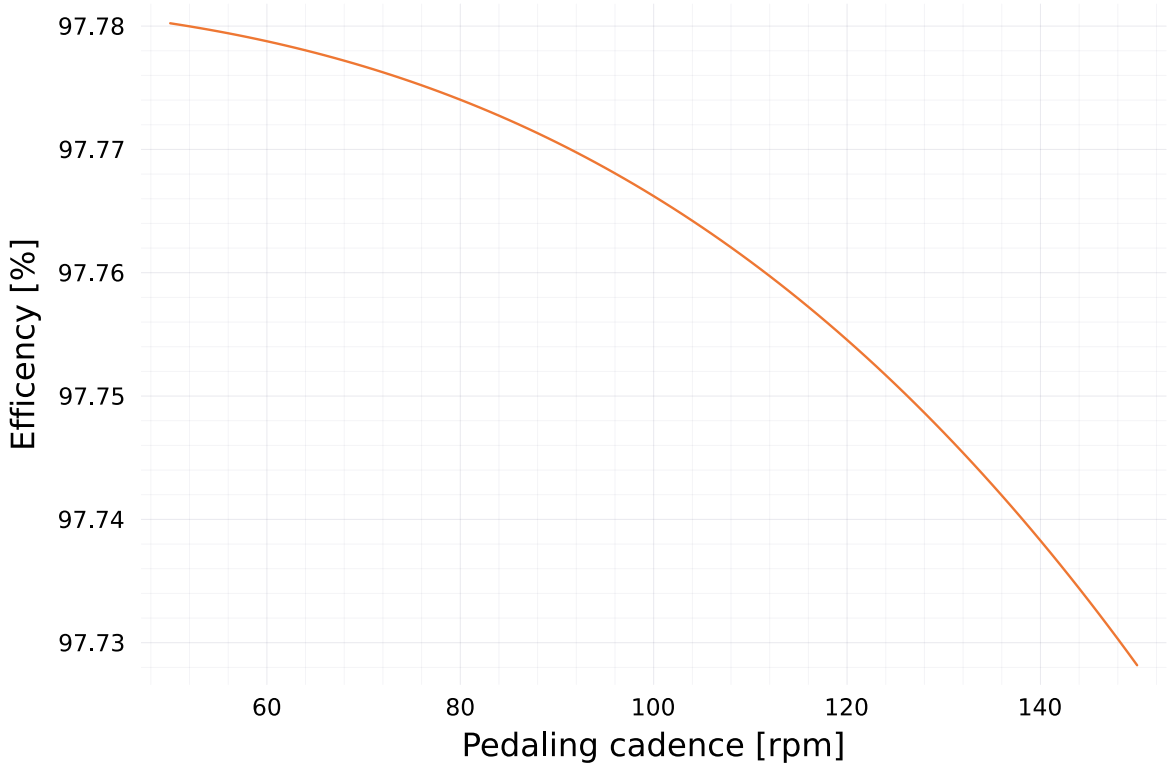

Figure 11: Efficiency as a function of pedaling cadence

Figure 11 shows that efficiency decreases when pedaling cadence is increased, for a fixed power input from the cyclist. However, increasing pedaling cadence from 50 to 150 rpm only decreases efficiency by 0.05%, which does not account for the observed behaviour in experiments.

Another common scenario in cycling is to keep pedaling cadence constant and modify power input. Figure 12 shows the change in efficiency as power input is increased, for a constant pedaling cadence of 80 rpm.

```
Pplot = 50:350

ηP = [ηT(i, fill(μ, 3), p, ρ, ψ, rR, [52, 21, 12, 12], ω, γ, m)*100 for i in Pplot]

plot(Pplot, ηP, label=false, xlabel="Power input [W]", ylabel="Efficiency [%]")
```

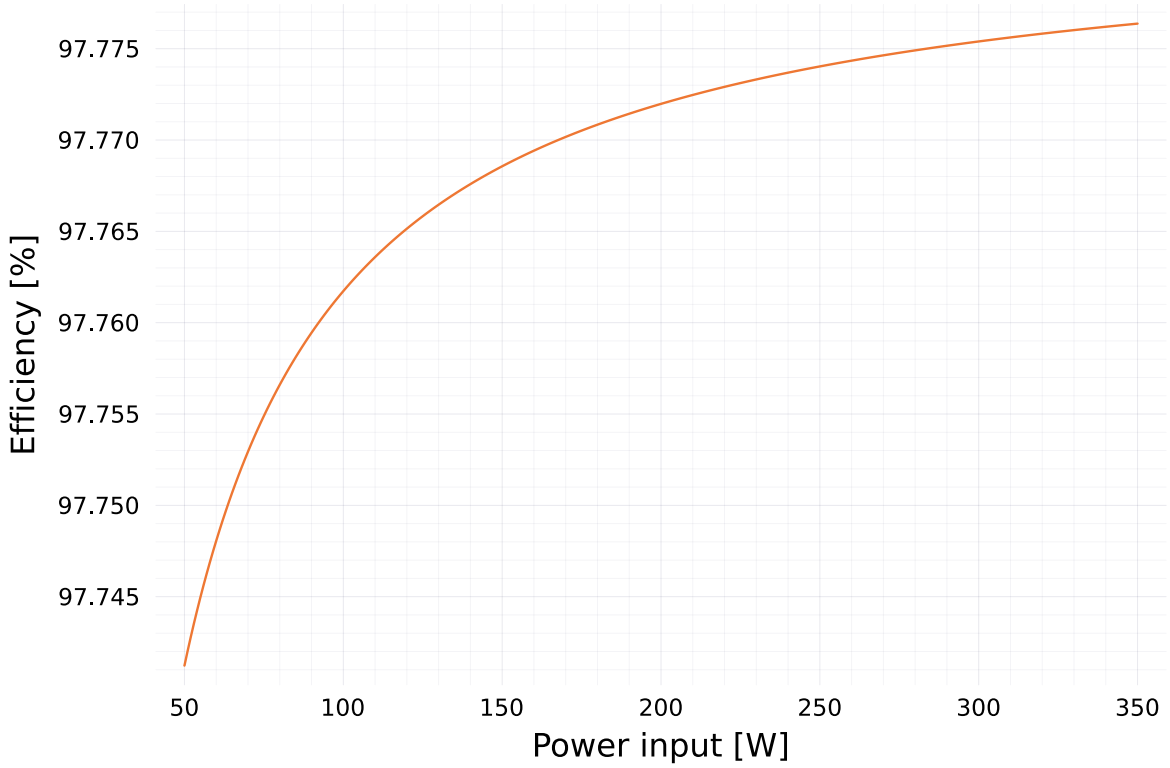

Figure 12: Efficiency as a function of power input, for a constant pedaling cadence of 80 rpm

Figure 12 shows that efficiency increases with load, which is an outcome that could not be observed in the original model, as stated by one of the authors in [9]. Moreover, this behaviour agrees with experimental measurements presented in [5] and [10]. However, it should be noted that increasing power input from 50 to 350 W only increased efficiency by 0.04%, which is much less than observed in practice.

Model validation

In order to determine whether the new modifications to the model increased its performance, the new model will also be validated against experimental data and compared with the original results. Table 2 presents these results.

Table 2: Modified frictional losses model validation

Pedaling cadence [rpm]	Measured efficiency [%]	Calculated efficiency [%]	Error [%]
40	97.8	97.78	0.02

Pedaling cadence [rpm]	Measured efficiency [%]	Calculated efficiency [%]	Error [%]
50	95.9	97.78	2.8
60	94.4	97.77	3.6
70	92.8	97.77	5.4
80	91.3	97.76	7.1
90	89.9	97.75	8.7

A comparison between the results presented in Table 2 with those in Table 1 shows that the changes introduced to the model have reduced the experimental error by approximately 2% for all pedaling speeds. However, it is still observed that error increases with pedaling cadence. This is due to the fact that the predicted decrease in efficiency as a consequence of increased pedaling cadence is much less than the one observed in practice. In particular, increasing pedaling cadence from 40 to 90 rpm decreases efficiency by almost 8%, while the model predicts that this decrease is only 0.03%.

Discussion and Conclusions

An analytical model to calculate a road bicycle's power transmission's system efficiency was developed and implemented computationally using the Julia programming language, which resulted in the creation of the library `BicycleEfficiency.jl`. Although this model was largely obtained from the literature (particularly [5]), improvements regarding the calculation of chain tension as a function of operating conditions and the consideration of the effects of chain tensioners were proposed in order to improve the model's accuracy.

The analysis performed on the model's outcomes and implications revealed a series of interesting facts about the behaviour of power losses and efficiency. Particularly, it was shown that efficiency and power losses are much more sensible to changes in rear sprocket size than front sprocket size. Figure 2 and Figure 8 show that increasing sprocket size reduces power loss and yields higher efficiencies, which is explained by a decrease in articulation angles, which in turn limits relative motion between chain pins and bushings during chain articulation. This is related to one of the main outcomes of the model, which indicates that nearly 90% of power losses come from friction betweeen chain pins and bushings, as it was shown in Figure 1 and Figure 7.

Regarding the modifications performed to the original model proposed in [5], it was observed they introduced several changes on the model's behaviour. In particular, a comparison between Figure 2 and Figure 8 reveals that the original model predicts a linear relationship between power losses and pedaling cadence, while the modified version of the model predicts that power losses are almost constant with respect to pedaling cadence (see also Figure 9). Related to this is the behaviour exhibited in Figure 11 and Figure 12 where it was shown that efficiency is no longer independent on pedaling cadence and power input (original model). Instead, efficiency

increases with power input and decreases with pedaling cadence, which is in agreement with experimental observations such as the ones found in [10].

Experimental validation of the models show that both models have a tendency to overestimate efficiencies, especially at high pedaling speeds, having an error of approximately 11% at 90 rpm for the original model. Changes introduced to the model increased its accuracy by nearly 2%, and allow the observation of the reduction of efficiency at higher pedaling cadences, whereas efficiency is predicted to remain constant in the original model. However, calculated efficiencies are still higher than their experimental counterparts, and the predicted decrease of efficiency at higher pedaling cadences is much smaller than observed.

Given that predicted efficiencies are higher than observed, even after introducing the adjustments mentioned above, it is reasonable to conclude that there must be another source of power loss apart from friction. This was also identified in [5], which led to measurements of energy losses using thermal cameras. Although these measurements are not explicitly included in the article, it is mentioned that energy losses determined with this method agree with model predictions, which supports the idea that there is another source of energy dissipation. Works such as [9] and [6] developed models for energy losses due to elastic deformation and impact. Future work on this area should focus on incorporating these results into the model and evaluating it's accuracy. In particular, it would be interesting to evaluate if these new sources of power loss can account for the reduction of efficiency at higher pedaling cadences, which appears to be the main weak point of the model presented here.

Appendix A: chain drive parameters used in calculations

Table 3 presents the parameters involved in the models implemented and the values used for calculations. The values which are not associated to a reference come from measurements performed by the author on a commercially available road bicycle.

Table 3: Chain drive parameters

Parameter	Symbol	Units	Value
Friction coefficient	μ	-	0.09 [5]
Chain pitch	p	mm	12.22
Chain pin radius	ρ	mm	1.13
Chain roller radius	R_r	mm	2.5
Chain misalignment angle	γ	deg	1 [5]
Free chain tension	T_0	N	300 [5]
Roller rotation angle	ψ	deg	90 [5]
Chain linear density	m	kg/m	1.52 [8]
Cyclist power input	P_{in}	W	250

References

[1] M. Angulo, A. Polanco, and L. Muñoz, "Influence of the cyclist's characteristics on the optimal pacing strategy for an ascending road," in *International design engineering technical conferences and computers and information in engineering conference*, 2021, vol. 85369, p. V001T01A012.

[2] S. D. Roa Melo *et al.*, "Bicycle change strategy for cycling uphill time-trial races," 2018.

[3] N. F. Almario Ramos *et al.*, "Generación de una estrategia de ritmo para una etapa ciclística," 2021.

[4] A. P. Polanco, L. E. Muñoz, A. Doria, and D. R. Suarez, "Selection of posture for time-trial cycling events," *Applied Sciences*, vol. 10, no. 18, p. 6546, 2020.

[5] J. B. Spicer, C. J. K. Richardson, M. J. Ehrlich, J. R. Bernstein, M. Fukuda, and M. Terada, "Effects of Frictional Loss on Bicycle Chain Drive Efficiency ," *Journal of Mechanical Design*, vol. 123, no. 4, pp. 598–605, Jun. 1999, doi: 10.1115/1.1412848.

[6] S.-P. Zhang and T.-O. Tak, "Efficiency estimation of roller chain power transmission system," *Applied Sciences*, vol. 10, no. 21, 2020, doi: 10.3390/app10217729.

[7] M. Kidd, N. Loch, and R. Reuben, "Experimental examination of bicycle chain forces," *Experimental mechanics*, vol. 39, no. 4, pp. 278–283, 1999.

[8] H. Rothbart and T. H. Brown, *Mechanical design handbook, measurement, analysis, and control of dynamic systems*. McGraw-Hill Education, 2006.

[9] J. B. Spicer, "Effects of the Nonlinear Elastic Behavior of Bicycle Chain on Transmission Efficiency," *Journal of Applied Mechanics*, vol. 80, no. 2, Jan. 2013, doi: 10.1115/1.4007431.

[10] E. R. Burke, *High-tech cycling*, Second Edition. Champaign, Ill: Human Kinetics, 2003.